Thanongsaksrikul J, Srimanote P, Maneewatch S, Choowongkomon K, Tapchaisri P, Makino S-I, Kurazono H, Chaicumpa W	A V_HH that neutralizes the zinc-metalloproteinase activity of botulinum neurotoxin type A.	J Biol Chem	285	9657-66	2010
Akada JK, Aoki H, Torigoe Y, Kitagawa T, Kurazono K, Hoshida H, Nishikawa J, Terai S, Matsuzaki M, Hirayama T, Nakazawa T, Akada R, Nakamura K	*Helicobacter pylori* CagA inhibits endocytosis of cytotoxin VacA in host cells.	Dis Model Mech	3	605-17	2010
Tamamura Y, Uchida I, Tanaka K, Okazaki H, Tezuka S, Hanyu H, Kataoka N, Makino S, Kishima M, Kubota T, Kanno T, Hatama S, Ishihara R, Hata E, Yamada H, Nakaoka Y, Akiba M	Molecular epidemiology of *Salmonella enterica* serovar Typhimurium isolates from cattle in Hokkaido, Japan: evidence of clonal replacement and characterization of the disseminated clone.	Appl Environ Microbiol	77	1739-50	2011
Matsui T, Takita E, Sato T, Aizawa M, Ki M, Kadoyama Y, Hirano K, Kinjo S, Asao H, Kawamoto K, Kariya H, Makino SI, Hamabata T, Sawada K, Kato K.	Production of double repeated B subunit of Shiga toxin 2e at high levels in transgenic lettuce plants as vaccine material for porcine edema disease.	Transgenic Res		Epub Oct 24	2010
江崎孝行	感染症法下での高度病原体の分譲活動と輸送方法の課題	Microbiol Cult Coll	26	127-9	2010
大楠清文、江崎孝行	核酸増幅法による感染症の診断	日本臨牀	68	501-5	2010

江崎孝行	ブルセラ症と炭疽	公衆衛生	75	19-22	2010
Ando S, Kurosawa M, Sakata A, Fujita H, Sakai K, Sekine M, Katsumi M, Saitou W, Yano Y, Takada N, Takano A, Kawabata H, Hanaoka N, Watanabe H, Kurane I, Kishimoto T	Human R. heilongjiangensis Infection, Japan	Emerg Infect Dis	16	1306-8	2010
Takeshita N, Imoto K, Ando S, Yanagisawa K, Ohji G, Kato Y, Sakata A, Hosokawa N, Kishimoto T	Murine typhus in two travelers returning from Bali, Indonesia: an under diagnosed disease	J Travel Med	17	356-8	2010
Yoshii K, Mottae K, Omori-Urabe Y, Chiba Y, Seto T, Sanada T, Maeda J, Obara M, Ando S, Ito N, Sugiyama M, Sato H, Fukushima H, Kariwa H, Takashima I	Epizootiological study of tick-borne encephalitis virus infection in Japan	J Vet Med Sci		Epub Nov 2	2010
Kuroda M, Serizawa M, Okutani A, Sekizuka T, Banno S, Inoue S	Genome-wide single nucleotide polymorphism typing method for identification of *Bacillus anthracis* species and strains among *B. cereus* group species.	J Clin Microbiol	48(8)	2821-9 Epub 2010 Jun 16	2010
Serizawa M, Sekizuka T, Okutani A, Banno S, Sata T, Inoue S, Kuroda M	Genomewide screening for novel genetic variations associated with ciprofloxacin resistance in *Bacillus anthracis*.	Antimicrob Agents Chemother	54(7)	2787-92 Epub 2010 Apr 12	2010

Jpn. J. Infect. Dis., 63, 36-40, 2010

Original Article

LAMP Using a Disposable Pocket Warmer for Anthrax Detection, a Highly Mobile and Reliable Method for Anti-Bioterrorism

Ben Hatano[1,3], Takayuki Maki[3], Takeyuki Obara[3], Hitomi Fukumoto[1,3], Kohsuke Hagisawa[3], Yoshitaro Matsushita[3], Akiko Okutani[2], Boldbaastar Bazartseren[2], Satoshi Inoue[2], Tetsutaro Sata[1], and Harutaka Katano[1]*

[1]Department of Pathology and [2]Department of Veterinary Science, National Institute of Infectious Diseases, Tokyo 162-8640; and [3]Military Medicine Research Unit, Japan Ground Self Defense Force, Tokyo 158-0098, Japan

(Received September 29, 2009. Accepted December 3, 2009)

SUMMARY: A quick, reliable detection system is necessary to deal with bioterrorism. Loop-mediated isothermal amplification (LAMP) is a DNA amplification method that can amplify specific DNA fragments in isothermal conditions. We developed a new highly mobile and practical LAMP anthrax detection system that uses a disposable pocket warmer without the need for electricity (pocket-warmer LAMP). In our tests, the detection limit of the pocket-warmer LAMP was 1,000 copies of *Bacillus anthracis pag* and *capB* gene fragments per tube. The pocket-warmer LAMP also detected *B. anthracis* genes from DNA extracted from 0.1 volume of a *B. anthracis* colony. The lower detection limit of the pocket-warmer LAMP was not significantly different from that of a conventional LAMP using a heat block, and was not changed under cold (4°C) or warm (37°C) conditions in a Styrofoam box. The pocket-warmer LAMP could be useful against bioterrorism, and as a sensitive, reliable detection tool in areas with undependable electricity infrastructures.

INTRODUCTION

Anthrax, a lethal disease in humans, is caused by *Bacillus anthracis*. Although natural cases of anthrax are rare in humans, the threat of bioterrorism using *B. anthracis* has increased (1). To deal with this possibility, a rapid, reliable detection system is necessary. Several detection systems, such as PCR, have been developed, but almost all of them require heavy, stationary equipment (2). Highly mobile detection systems for anthrax have been developed that rely on immunochromatography methods, such as the Sensitive Membrane Antigen Rapid Test (SMART) and the Antibody-based Lateral Flow Economical Recognition Ticket (ALERT) (2). However, their sensitivity is not sufficient for reliable detection (2). Here, we describe a sensitive and highly mobile anthrax detection system, combining the loop-mediated isothermal amplification (LAMP) method with a disposable pocket warmer, designated as "pocket-warmer LAMP." LAMP is a recently developed DNA amplification method with high specificity, efficiency, and speed under isothermal conditions (3,4). LAMP requires a set of four primers (B3, F3, BIP, and FIP) that recognize six distinct sequences (B1, B2, B3, F1, F2, and F3) in the target DNA. The use of the four primers enhances the specificity of DNA amplification. The most significant advantage of LAMP is that the reaction proceeds under isothermal conditions. Since the amplification requires a constant temperature range of 60–65°C for 1 h, LAMP requires only a heat blocker as equipment. This is a big advantage in developing countries or laboratories equipped with no thermal cycler. Disposable pocket warmers are a well-known winter commodity in Japan. They cost less than 100 yen each and are available anywhere in Japan. In this study, we used a disposable pocket warmer as a heat source for the LAMP reaction. We evaluated the lower detection limit of the pocket-warmer LAMP for anthrax detection and also investigated the influences of environmental temperature and the differences among pocket warmers made by different manufacturers.

*Corresponding author: Mailing address: Department of Pathology, National Institute of Infectious Diseases, Toyama 1-23-1, Shinjuku-ku, Tokyo 162-8640, Japan. Tel: +81-3-5285-1111 ext. 2627, Fax: +81-3-5285-1189, E-mail: katano@nih.go.jp

MATERIALS AND METHODS

Disposable pocket warmers: Disposable pocket warmers were purchased at drugstores in Japan. Four different pocket warmers made by different companies (A–D) were used. According to the manufacturers' information, these pocket warmers reach 68°C at maximum, and the average temperature during a 12-h period is 53°C.

Bacterial strains: Three strains of *B. anthracis*—BA101, BA103, and BA104—were used (5–7). BA101 was previously used as a vaccine strain for cattle and horses in Japan. BA103 was isolated from dairy cattle in Miyagi Prefecture in 1991. BA104 was isolated from swine in Shizuoka Prefecture in 1982. *B. thuringiensis* GTC2847, *B. cereus* GTC419, *B. cereus* GTC1777, and *B. cereus* GTC2826 provided by the National Bio Resource Project, Gifu University Graduate School of Medicine, and *B. subtilis* NIID-1 by the National Institute of Infectious Diseases were used as controls.

Culture and DNA extraction: One colony of *B. anthracis* was cultured in 2 mL of trypticase soy broth at 37°C overnight (8). DNA was extracted from 1 ml of the overnight-cultured *B. anthracis* using the phenol and chloroform method. Another 1 ml was serially diluted and plated on a trypticase soy agar plate. After overnight culture, colonies were counted to determine colony formation units (CFUs).

Preparation of control DNA: To determine the lower detection limit of LAMP, *pag* and *capB* genes from *B. anthracis* were amplified from BA101 using F3 and B3 primers (9).

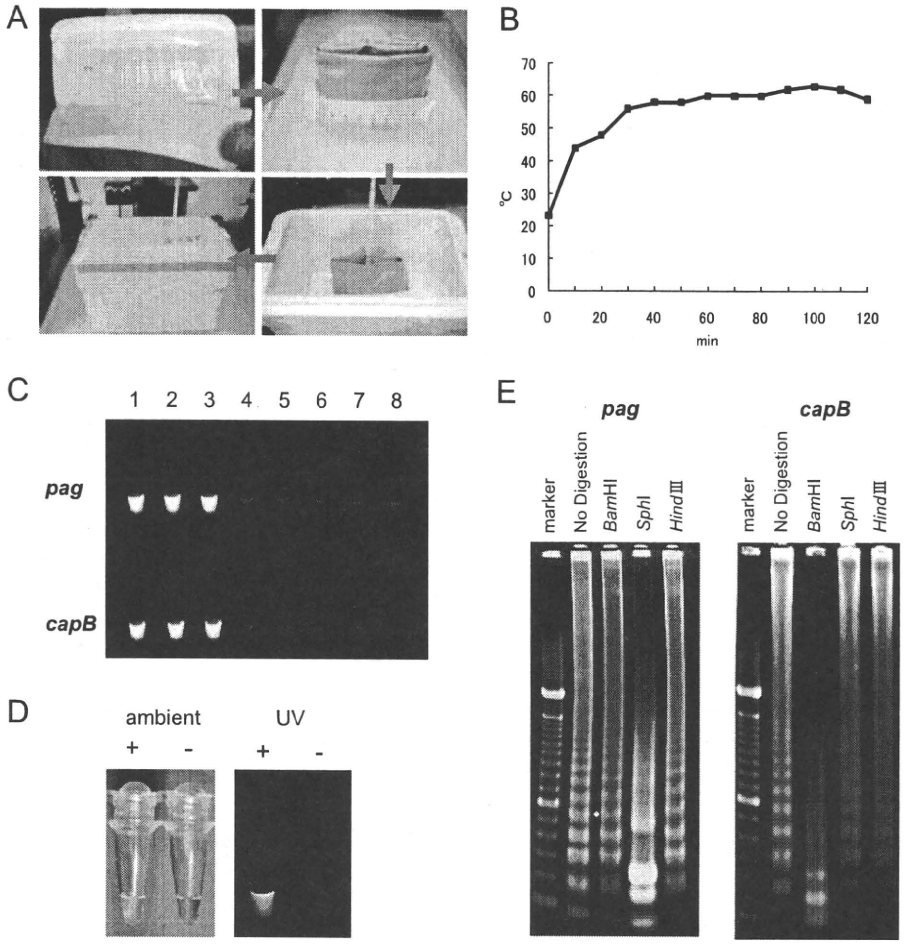

Fig. 1. Establishment of pocket-warmer LAMP. (A) The procedure of pocket-warmer LAMP. Reaction tubes were placed on a pocket warmer (upper left panel), folded and surrounded by a paper towel (upper right panel), and put into Styrofoam box with a thermometer (lower panels). The tubes were incubated for 90 min. (B) Temperature of pocket warmers in Styrofoam box. The temperature reached to 60°C in about 30 min and stayed at about 60°C for 90 min. (C) Fluorescence image of pocket-warmer LAMP products in tubes using UV light exposure. Ten ng of DNA was applied per tube. 1, *B. anthracis* BA101; 2, *B. anthracis* BA103; 3, *B. anthracis* BA104; 4, *B. thuringiensis* GTC2847; 5, *B. cereus* GTC419; 6, *B. cereus* GTC1777; 7, *B. cereus* GTC2826; 8, *B. subtilis* NIID-1. (D) Color image of pocket-warmer LAMP products under ambient light (left) and UV light (right). LAMP product showed green color under ambient light. (+) and (−) indicate a positive and negative sample, respectively. (E) Agarose gels electrophoresis of LAMP products digested with restriction enzymes. The LAMP products of *pag* or *capB* were digested with *Bam*HI, *Sph*I, and *Hind*III. The left lane in each gel is a 100-bp ladder molecular weight marker.

The reaction mixture for the PCR consisted of 1 μl *B. anthracis* genomic DNA, 1 μmol/L of each primer (F3, B3), 12.5 μl 2 × high-fidelity PCR master mix (Roche Diagnostics, Boehringer Mannheim, Mannheim, Germany) and enough water for a final volume of 25 μl. Primary amplification conditions were 94°C for 2 min; 35 cycles at 94°C for 30 s, annealing at 55°C for 30 s, extension at 72°C for 30 s; and final extension at 70°C for 10 min. The PCR products were purified with a gel extraction kit (Qiagen, Hilden, Germany) and their copy numbers calculated based on their molecular weights. The PCR product was then used to make standard dilutions (10^0–10^8 copies/μl) to evaluate the lower detection limit of the LAMP process.

LAMP: The *pag* and *capB* genes of *B. anthracis* were amplified with a loopamp DNA amplification kit (Eiken Chemical, Tochigi, Japan) using primers published previously (9). Each 25-μl reaction mixture contained 1.6 μM each of FIP and BIP, 0.2 μM each of F3 and B3, 0.8 μM each of LF and LB, 2 × reaction mixture (12.5 μl), *Bst* DNA polymerase (1 μl), fluorescence detection reagent (Eiken Chemical, 1 μl), 3.5 μl distilled water, and 1 μl sample. Reaction tubes were incubated in a heat blocker (GeneAmp 9700; Applied Biosystems, Foster City, Calif., USA) or a pocket warmer. In the heat blocker, tubes were incubated at 60°C for 60 min. For the pocket-warmer LAMP, tubes were sandwiched in a twofold pocket warmer surrounded by a paper towel and put in a Styrofoam box for 90 min (Fig. 1A). To study the influence of environmental temperature, we operated the pocket-warmer LAMP in cold conditions (4°C) or hot conditions (37°C), with or without a Styrofoam box. The positive LAMP reactions were checked under both ultraviolet (UV) light and ambient light. LAMP products were subjected to electrophoresis on a 2% agarose gel. The gels were visualized under UV light after ethidium bromide staining. In some experiments, LAMP products of *pag* and *capB* were purified with a PCR purification kit (Qiagen), digested with *Bam*HI, *Sph*I, and *Hind*III (New England Biolabs, Ipswich, Mass., USA), and subjected to electrophoresis on a 2% agarose gel.

RESULTS

Establishment of pocket-warmer LAMP: The LAMP method requires constancy of temperature at about 60°C for 60 min in order to amplify DNA. To know if a commercially

available disposable pocket warmer is able to maintain that temperature for the appropriate period, we monitored the temperature of a pocket warmer in a Styrofoam box first. It reached 58°C in 30 min and stayed around 60°C for more than 60 min (Figs. 1A and 1B). We then conducted the LAMP reaction with a pocket warmer. Observation under UV light revealed that the pocket-warmer LAMP amplified the *pag* and *capB* gene fragments in DNA samples from three strains of *B. anthracis*–BA101, BA103, and BA104–but not from strains of *B. thuringiensis*, *B. cereus*, and *B. subtilis* for 90 min (Fig. 1C). In addition, the amplification for *B. anthracis* was also observed as a change of color under ambient light (Fig. 1D). To confirm the specificity of the pocket-warmer LAMP, the LAMP products of *B. anthracis* were digested with restriction enzymes. Each target gene of *pag* and *capB* LAMP has a restriction enzyme site for *Sph*I and *Bam*HI, respectively. A few bands sized around 200 bp were observed in the lane of *Sph*I (*pag*) and *Bam*HI (*capB*)-digested LAMP products, while smear and ladder bands were seen in the other lanes (Fig. 1E). Similar results were observed in enzyme-digested LAMP products with both the heat block and pocket warmer (data not shown). These data indicate specific amplification for *B. anthracis* by the pocket-warmer LAMP.

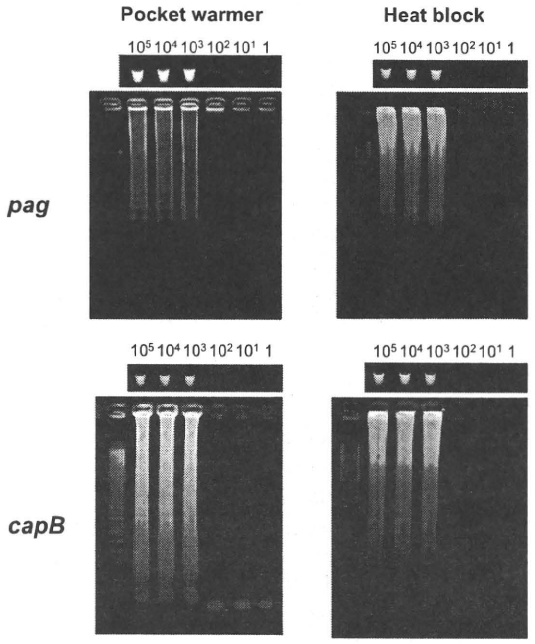

Fig. 2. Lower detection limit of LAMP using pocket warmer or heat block. Serial dilutions of *pag* and *capB* gene fragments were examined to determine the lower detection limit of the assay. The numbers in the top of upper panels are copy numbers of the target gene. Fluorescence image of tubes using UV light exposure (upper panels) and agarose gels electrophoresis (lower panels) are shown. The left lane on each gel is a 100-bp laddered molecular weight marker.

Comparison of lower detection limit with conventional LAMP: To compare the lower detection limit and quality of the pocket warmer LAMP with the conventional LAMP using a heat block, diluted DNA fragments of *pag* and *capB* were examined by both methods. Exposure to UV light showed that the detection limit of both methods was 1,000 copies of the *pag* and *capB* genes per tube (Fig. 2). Gel electrophoresis demonstrated that the pocket-warmer LAMP produced a pattern of electrophoresis similar to that of the conventional LAMP. We then investigated whether or not the pocket-warmer LAMP could amplify the *pag* and *capB* genes from DNA samples extracted from *B. anthracis* at a lower detection limit similar to that of conventional LAMP. The pocket-warmer LAMP amplified the *pag* and *capB* genes from DNA extracted from 0.1 and 1.0 volume of CFU, while conventional LAMP amplified them from 0.1 CFU (Fig. 3). These data suggest no significant difference in the lower detection limit between the conventional and pocket-warmer methods.

Conditions of the pocket-warmer LAMP: To evaluate the effects of environmental temperature on this method's performance, we used the pocket-warmer LAMP under cold (4°C) or warm (37°C) conditions, with or without a Styrofoam box (Table 1). With a Styrofoam box, the pocket-warmer LAMP consistently amplified the *pag* and *capB* genes from DNA containing 1,000 copies of the genes under both cold and warm conditions. However, without the Styrofoam box, the pocket-warmer LAMP did not amplify the genes from DNA containing 10^8 copies of the *pag* and *capB* genes. When we put these LAMP reaction mixtures with a pocket warmer into a pocket of pants worn by one of the experimenters, the

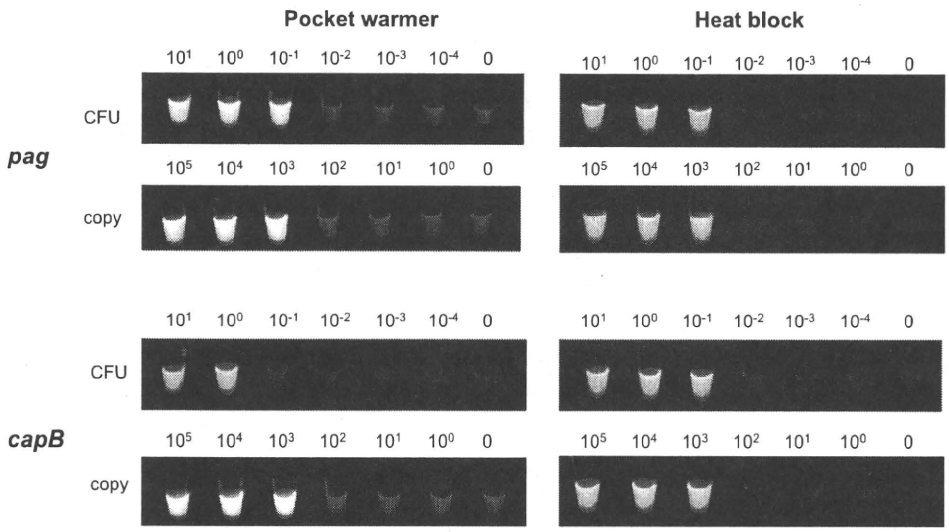

Fig. 3. Comparison of CFUs and copy numbers in pocket-warmer LAMP (left panels) and conventional LAMP using a heat block (right panels). Serial dilutions of *pag* and *capB* gene fragments and DNA extracted from *B. anthracis* were examined to determine the lower detection limit of the assay. Fluorescence images using UV light exposure are shown.

Table 1. Condition of pocket-warmer LAMP

	Pocket warmer							
	4°C		RT		37°C		In pocket	Heat block
Styrofoam box	+	−	+	−	+	−	−	
pag	10^3	$>10^8$	10^3	10^3	10^3	10^3	$>10^8$	10^3
capB	10^2	$>10^8$	10^3	10^3	10^3	10^3	$>10^8$	10^3

10^1–10^8 copies of the *pag* and *capB* genes were examined. Copy numbers detected in LAMP are shown.
RT, room temperature.

Table 2. Comparison of pocket warmers

	Pocket warmer				Heat block
Company	A	B	C	D	
pag	10^3	10^3	10^3	10^3	10^3
capB	10^3	10^3	10^3	10^3	10^3

10^1–10^8 copies of *pag* and *capB* genes were examined. Copy numbers detected in LAMP are shown.

pag and *capB* genes were not amplified even from DNA containing 10^8 copies. These data suggest that the pocket-warmer LAMP should be used in a Styrofoam box. To verify the differences among commercially available pocket warmers from different manufacturers, we tested the performance of pocket warmers from four different companies. All of them had similar abilities and showed no significant differences in lower detection limit (Table 2).

DISCUSSION

In the present study, we established the pocket-warmer LAMP, a new, highly mobile and sensitive method for anthrax detection. This system is able to amplify the *pag* and *capB* genes of *B. anthracis* from DNA containing 1,000 copies corresponding to 0.1 volume of a CFU. It takes less than 90 min and can be detected with ambient light.

The most significant advantage of this pocket-warmer LAMP is its high mobility. For bioterrorism or similar emergencies, rapid and accurate detection are necessary. So far, several early detection systems for bioterrorism agents have been developed (2). However, because almost all of them require at least heat blocks and a centrifuge, it is difficult to detect bioterrorism or other disease agents immediately at the scene of a suspected outbreak. If the detection system requires any equipment, samples must be shipped from the outbreak site to the laboratory where the equipment is. The pocket-warmer LAMP does not require any heavy equipment such as heat blockers or thermal cyclers. Moreover, it does not need any electric power. The pocket-warmer LAMP, therefore, can reduce transit time and produce a rapid detection. Anti-bioterrorism methods developed thus far are not especially applicable to events happening in undeveloped areas or disaster sites in which electricity infrastructures are inadequate or destroyed. In addition to its mobility, it is also inexpensive. Although a DNA amplification kit and specific primers are required, pocket warmers are disposable and typically cost less than 100 yen each. Such low cost is a big advantage, especially in developing countries.

LAMP's specificity and sensitivity are similar to those of PCR (3). Because the four specific primers and two loop-primers used in LAMP recognize six different regions of the target genes, these primers enhance the specificity of the reaction. The specificity and sensitivity of conventional LAMP using the primers that we used in the present study have already been examined by a previous study (9). It detected 10 spores of *B. anthracis* per tube (9). This lower detection limit is higher than conventional PCR (at about 100 spores per tube). Our results showed the pocket-warmer LAMP's lower detection limit is similar to that of conventional LAMP, suggesting that its lower detection limit might be 10 spores per tube.

Condition experiments revealed that the pocket-warmer LAMP should be used only under certain conditions. To obtain the target temperature of the pocket-warmer LAMP, it is important to insulate it from environmental temperatures. We used a Styrofoam box to isolate the pocket warmers from the environment, which worked very well. It should be noted that the LAMP reaction did not work under cold conditions without a Styrofoam box or in a pants pocket.

To establish an entire mobile detection system for anthrax, we have to think about other steps. The procedure for DNA extraction usually requires a heat block and a centrifuge. However, a previous study demonstrated that DNA samples extracted from *B. anthracis* with the boiling method (95–100°C for 30 min in sterile water) were sufficient for LAMP (9). Moreover, DNA extraction kits using magnetic beads do not require any centrifuge or heat block. In addition, DNA amplification reagents for LAMP should be shipped under cold conditions to the bioterrorism or outbreak site. The method of collecting samples from the environment is another concern for the establishment of the entire system. Thus, although further experimentation and development are necessary to resolve these problems, the pocket-warmer LAMP will contribute to rapid, reliable anti-bioterrorism responses. This technique also has the potential to provide detection tools for infectious diseases in areas that do not have functional electricity infrastructures.

ACKNOWLEDGMENTS

The authors thank Dr. Akio Yamada, Department of Veterinary Science, National Institute of Infectious Diseases, for his helpful discussion.

This study was supported by the Health and Labour Sciences Research Grants on Emerging and Re-emerging Infectious Diseases (to TS, No. H20-Shinko-Ippan-006) from the Ministry of Health, Labour and Welfare of Japan.

REFERENCES

1. Wang, J.Y. and Rochrl, M.H. (2005): Anthrax vaccine design: strategies to achieve comprehensive protection against spore, bacillus, and toxin. Med. Immunol., 4, 4.
2. Bravata, D.M., Sundaram, V., McDonald, K.M., et al. (2004): Evaluating detection and diagnostic decision support systems for bioterrorism response. Emerg. Infect. Dis., 10, 100–108.
3. Nagamine, K., Hase, T. and Notomi, T. (2002): Accelerated reaction by loop-mediated isothermal amplification using loop primers. Mol. Cell. Probes, 16, 223–229.
4. Notomi, T., Okayama, H., Masubuchi, H., et al. (2000): Loop-mediated isothermal amplification of DNA. Nucleic Acids Res., 28, E63.

5. Fujita, O., Inoue, S., Tatsumi, M., et al. (2002): Amplification of irrelevant sequence from *Bacillus subtilis* using a primer set designed for detection of the *pag* gene of *Bacillus anthracis*. Jpn. J. Infect. Dis., 55, 99–100.
6. Inoue, S., Noguchi, A., Tanabayashi, K., et al. (2004): Preparation of a positive control DNA for molecular diagnosis of *Bacillus anthracis*. Jpn. J. Infect. Dis., 57, 29–32.
7. Okutani, A., Sekizuka, T., Boldbaatar, B., et al.: Phylogenetic typing of *Bacillus anthracis* isolated in Japan by the multiple locus variable-number tandem repeats and the comprehensive single nucleotide polymorphism. J. Vet. Med. Sci. (in press).
8. Sanz, P., Teel, L.D., Alem, F., et al. (2008): Detection of *Bacillus anthracis* spore germination in vivo by bioluminescence imaging. Infect. Immun., 76, 1036–1047.
9. Qiao, Y.M., Guo, Y.C., Zhang, X.E., et al. (2007): Loop-mediated isothermal amplification for rapid detection of *Bacillus anthracis* spores. Biotechnol. Lett., 29, 1939–1946.

Jpn. J. Infect. Dis., 63, 52-54, 2010

Short Communication

Virus Detection Using Viro-Adembeads, a Rapid Capture System for Viruses, and Plaque Assay in Intentionally Virus-Contaminated Beverages

Ben Hatano[1,2], Asato Kojima[1], Tetsutaro Sata[1], and Harutaka Katano[1]*

[1]*Department of Pathology, National Institute of Infectious Diseases, Tokyo 162-8640; and*
[2]*Military Medicine Research Unit, Japan Ground Self Defense Force, Tokyo 158-0098, Japan*

(Received July 28, 2009. Accepted November 12, 2009)

SUMMARY: Intentional contamination of beverages with microbes is one type of bioterrorist threat. While bacteria and fungus can be easily collected by a centrifuge, viruses are difficult to collect from virus-contaminated beverages. In this study, we demonstrated that Viro-Adembeads, a rapid-capture system for viruses using anionic polymer-coated magnetic beads, collected viruses from beverages contaminated intentionally with vaccinia virus and human herpesvirus 8. Real-time PCR showed that the recovery rates of the contaminated viruses in green tea and orange juice were lower than those in milk and water. Plaque assay showed that green tea and orange juice cut the efficiency of vaccinia virus infection in CV-1 cells. These results suggest that the efficiency of virus detection depends on the kind of beverage being tested. Viro-Adembeads would be a useful tool for detecting viruses rapidly in virus-contaminated beverages used in a bioterrorist attack.

Intentional contamination of beverages with microbes is a relatively easy way for terrorists to transmit microbes to anonymous persons and to induce a public panic. Although the few incidents of intentional viral contamination of drinks in Japan to date have not been real bioterrorist attacks, a similar act as a form of terrorism could be devastating. Therefore, an efficient and rapid detection system to detect microbes in contaminated drinks should be developed as an anti-bioterrorism tool. While bacteria and fungi can be easily collected by a centrifuge, viruses are difficult to collect from virus-contaminated beverages. An ultracentrifuge is a useful tool for virus collection in liquid samples, but not every laboratory is equipped with an ultracentrifuge. In addition, virus concentration with an ultracentrifuge usually takes more than 3 h.

Viro-Adembeads (Ademtech, Pessac, France) are recently developed magnetic beads intended for capturing viruses in liquid samples. They are specifically designed to function in virus-containing cell culture media (1,2). An anionic polymer coating on the magnetic beads binds to the surface of virus particles electrically; the complex of virus and beads can then be collected using a magnet. In the present study, we examined the capacity of Viro-Adembeads to collect viruses in virus-contaminated beverages. We also investigated whether the kind of beverage tested affected the efficiency of virus detection in this manner.

To represent intentional contamination of beverages with viruses, we mixed a solution containing two viruses with beverages. Human herpesvirus 8 (HHV-8) and vaccinia virus (LC16m8) were collected as reported previously (3,4). Milk, green tea, water, orange juice, and barley tea were purchased from a convenience store in Tokyo. To create virus-contaminated beverages, we added 0.1 mL of virus solution containing 1×10^7 copies of HHV-8 or vaccinia virus into 0.9 mL of beverages in 1.5-mL tubes. Each virus-contaminated beverage was serially diluted ×10 with the beverage at each stage, to ×10,000. If a terrorist was to contaminate beverages with viruses in a food store, the period of incubation would probably be from 5 min to several days; for our sample incubation time, we incubated the contaminated beverages for 1 h. To collect viruses from virus-contaminated beverage samples, we then used Viro-Adembeads according to the manufacturer's instructions. Briefly, 25 μL of washed Viro-Adembeads solution was added to each 1-mL aliquot of a virus-contaminated beverage sample. After 20 min of agitation at room temperature, the Viro-Adembeads were collected with a magnet. The beads were then washed with PBS twice. DNA was directly extracted from the beads with a DNA extraction kit (DNeasy; Qiagen, Hilden, Germany). The DNA was dissolved in 100 μL of water. Virus copy numbers were measured with a TaqMan Real-Time PCR (Applied Biosystems, Foster City, Calif., USA) as previously described (5). To detect HHV-8, we amplified ORF-26 using a previously reported probe and primer set (6). To detect vaccinia virus, we used a consensus probe and primer set targeting the F2R region of orthopoxvirus as follows: forward primer 5′-gatctagttttcagcacggtggta-3′, reverse primer 5′-cagatatatgattggatgtagaacaccat-3′, and probe 5′-FAM-agaggtggaggaatttatagatgatggaagacaagtt-TAMRA-3′. The recovery rate was calculated by the retrieved virus copy number with Viro-Adembeads, divided by the input virus copy number in 1 mL of each sample. The results of real-time PCR showed that the amount of collected virus was proportionally reduced as the sample was diluted (Figure 1A and 1B). Copies of HHV-8 and vaccinia virus were reduced almost one-tenth per dilution. However, copies of HHV-8 in ×100, ×1,000, and ×10,000 dilutions of green tea, and vaccinia virus in the ×10 dilution of green tea were extremely reduced. Although 34% of input HHV-8 was detected in the water sample, other beverages such as milk, orange juice, and green tea demonstrated lower recovery rates (Figure 1C). The recovery rate of HHV-8 with Viro-Adembeads was 39% in culture media (RPMI 1640 medium supplemented with 10% fatal bovine serum) containing the same amount of HHV-8 to the ×10 dilution, suggesting similar efficacy of virus collection with Viro-Adembeads between water and culture

*Corresponding author: Mailing address: Department of Pathology, National Institute of Infectious Diseases, Toyama 1-23-1, Shinjuku-ku, Tokyo 162-8640, Japan. Tel: +81-3-5285-1111 ext. 2627, Fax: +81-3-5285-1189, E-mail: katano@nih.go.jp

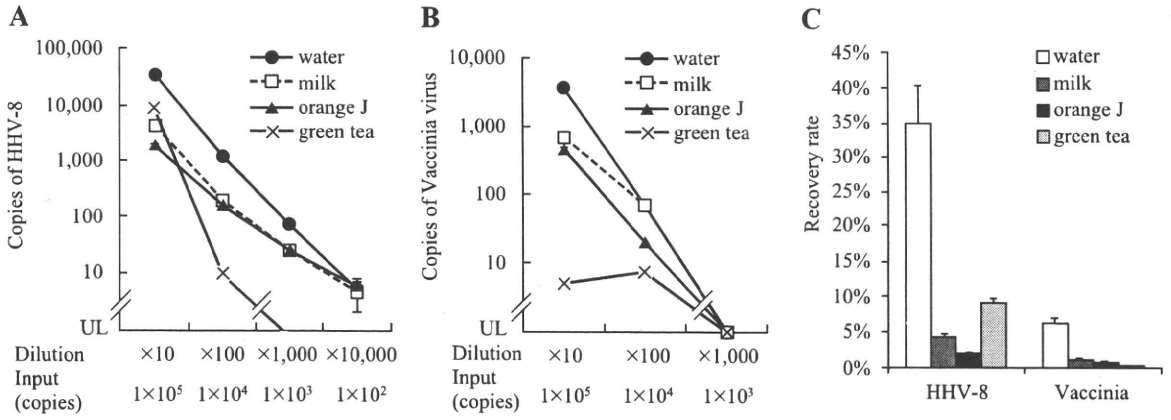

Fig. 1. HHV-8 and vaccinia virus detection using Viro-Adembeads. (A) Copies of HHV-8. (B) Copies of vaccinia virus. The *y*-axis indicates copy numbers of the virus in 1% of the extracted DNA. 'UL' indicates 'under limitation'. 'Dilution' and 'Input' under the *x*-axis indicate dilution factors and 1% of the virus copy numbers in 1 mL of each sample, respectively. (C) Recovery rates. Virus solutions were diluted ×10 with beverages; viruses were then recovered with Viro-Adembeads. Recovery rates were calculated based on the results of real-time PCR. Error bars indicate standard deviations.

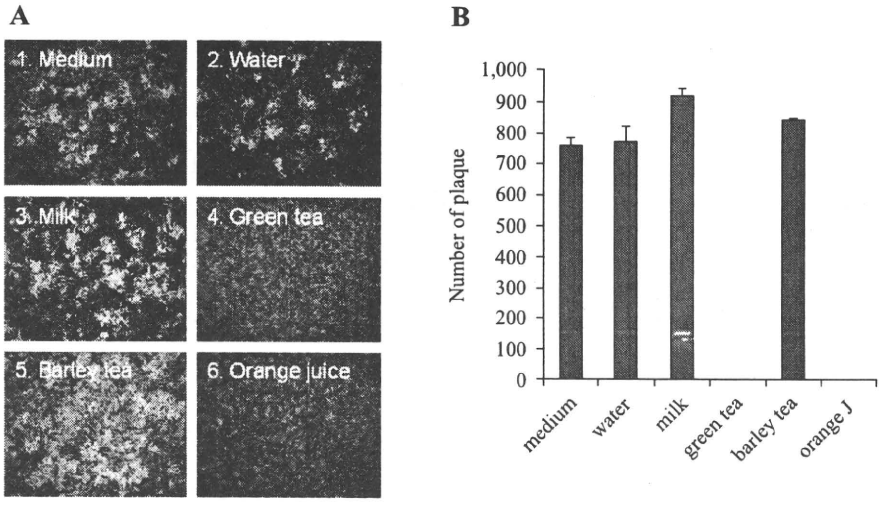

Fig. 2. Green tea and orange juice reduce the efficiency of vaccinia virus infection. (A) Microscopic view of plaques. (B) Numbers of plaque by vaccinia virus. Error bars indicate standard deviations.

media. Vaccinia virus was also recovered at low rates in all beverages. In both viruses, the recovery rates differed among beverages. For example, the recovery rates in milk, orange juice, and green tea were significantly lower than that in water. These results indicate that the efficiency of virus detection depends on the kind of beverage being tested.

To know whether the beverage type affects viral infectivity, we examined a plaque assay using vaccinia virus in the beverages, because it is difficult to perform a plaque assay in HHV-8 (7). Virus solution containing 10,000 plaque-forming units (pfu) was mixed with 1 mL of each beverage and incubated with rotation for 20 min. From these solutions, 100-μL samples were added to CV-1 cells with 1 mL of serum-free medium per well in a 6-well plate. The plaque assay showed that the number of plaques was dramatically reduced in green tea and orange juice (Figure 2). The plaque number in barley tea did not change from that of water and milk. These results suggested that green tea and orange juice reduced the infectivity of vaccinia virus. The pH conditions of the water, milk, orange juice, and green tea used in this experiment were pH 7.2, 6.8, 4.0, and 6.2, respectively, suggesting that acidity is not the only factor in reducing virus infectivity.

The results in the present study suggest that the type of beverage affects virus detection in virus-contaminated beverages and that Viro-Adembeads would be a useful tool for virus detection in virus-contaminated beverages. Our results clearly demonstrated that orange juice and green tea reduced virus infectivity of vaccinia virus. One of the reasons could be a low pH in orange juice, but other factors were unveiled. We checked pH conditions of several kinds of orange juice in a food store and found they ranged from pH 3.3 to pH 4.2, suggesting that the orange juice used in the present study was not special, at least with regard to its pH condition. Incubation of viruses with orange juice or green tea reduced not only the number of plaques in a plaque assay but also the copy numbers of the virus detected by a real-time PCR after virus collection, suggesting that orange juice and green tea affect the binding efficiency of viruses to Viro-Adembeads, in addition to reducing virus infectivity. No plaque was observed in any well of CV-1 cells with 10,000 pfu of vaccinia virus incubated with orange juice or green tea. On the other hand, we could detect the viruses from orange juice or green tea containing the same amount of viruses by Viro-adembeads and real-time PCR, although the recovery rate was low. These data indicated that Viro-adembeads and real-time PCR was more sensitive for detecting vaccinia virus in orange juice

and green tea than was the plaque assay.

The use of Viro-Adembeads is an easy method for collecting viruses from a virus-contaminated liquid. One of the merits of this method is its rapidity. In our experiment, it took about 30 min to collect viruses from virus-contaminated beverages, which is much quicker than the using the ultracentrifuge method. Another merit is that Viro-Adembeads can be used in liquid samples with some precipitation and turbidity, like milk and orange juice. Such precipitation and turbidity interfere with efficient isolation of viruses in any method using an ultracentrifuge. In addition, the use of Viro-Adembeads does not require any machine. Thus, although further studies are required to determine optimal techniques and conditions, Viro-Adembeads could be a useful tool for rapidly detecting viruses in virus-contaminated beverages.

ACKNOWLEDGMENTS

This study was supported by the Health and Labour Sciences Research Grants on Emerging and Re-emerging Infectious Diseases (to TS, No. H20-Shinko-Ippan-006) from the Ministry of Health, Labour and Welfare of Japan; and a grant for Research on Publicly Essential Drugs and Medical Devices from the Japan Health Sciences Foundation (to HK and TS, No. SAA4832).

REFERENCES

1. Sakudo, A., Baba, K., Tsukamoto, M., et al. (2009): Anionic polymer, poly(methyl vinyl ether-maleic anhydride)-coated beads-based capture of human influenza A and B virus. Bioorg. Med. Chem., 17, 752–757.
2. Sakudo, A. and Ikuta, K. (2008): Efficient capture of infectious H5 avian influenza virus utilizing magnetic beads coated with anionic polymer. Biochem. Biophys. Res. Commun., 377, 85–88.
3. Morikawa, S., Sakiyama, T., Hasegawa, H., et al. (2005): An attenuated LC16m8 smallpox vaccine: analysis of full-genome sequence and induction of immune protection. J. Virol., 79, 11873–11891.
4. Renne, R., Zhong, W., Herndier, B., et al. (1996): Lytic growth of Kaposi's sarcoma-associated herpesvirus (human herpesvirus 8) in culture. Nat. Med., 2, 342–346.
5. Asahi-Ozaki, Y., Sato, Y., Kanno, T., et al. (2006): Quantitative analysis of Kaposi sarcoma-associated herpesvirus (KSHV) in KSHV-associated diseases. J. Infect. Dis., 193, 773–782.
6. White, I.E. and Campbell, T.B. (2000): Quantitation of cell-free and cell-associated Kaposi's sarcoma-associated herpesvirus DNA by real-time PCR. J. Clin. Microbiol., 38, 1992–1995.
7. Fedorko, D.P., Preuss, J.C., Fahle, G.A., et al. (2005): Comparison of methods for detection of vaccinia virus in patient specimens. J. Clin. Microbiol., 43, 4602–4606.

Jpn. J. Infect. Dis., 63, 67-71, 2010

Short Communication

The First Autopsy Case of Pandemic Influenza (A/H1N1pdm) Virus Infection in Japan: Detection of a High Copy Number of the Virus in Type II Alveolar Epithelial Cells by Pathological and Virological Examination

Noriko Nakajima[1], Satoru Hata[2], Yuko Sato[1], Minoru Tobiume[1], Harutaka Katano[1], Keiko Kaneko[1], Noriyo Nagata[1], Michiyo Kataoka[1], Akira Ainai[3], Hideki Hasegawa[1,3], Masato Tashiro[3], Makoto Kuroda[4], Tamami Odai[5], Nobuyuki Urasawa[5], Tomoyoshi Ogino[6], Hiroaki Hanaoka[6], Masahide Watanabe[6], and Tetsutaro Sata[1]*

[1]Department of Pathology, [3]Influenza Virus Research Center, and [4]Pathogen Genomics Center, National Institute of Infectious Diseases, Tokyo 162-8640; and [2]Department of Clinical Laboratory, [5]Department of Cardiology, and [6]Department of Pathology, Nagano Red Cross Hospital, Nagano 380-8582, Japan

(Received December 15, 2009. Accepted January 5, 2010)

SUMMARY: We report the pathological and virological findings of the first autopsy case of the 2009 pandemic influenza (A/H1N1pdm) virus infection in Japan. A man aged 33 years with chronic heart failure due to dilated cardiomyopathy, mild diabetes mellitus, atopic dermatitis, bronchial asthma, and obesity died of respiratory failure and multiple organ dysfunction syndrome. Macroscopic examination showed severe plumonary edema and microscopically the lung sections showed very early exudative-stage diffuse alveolar damage (DAD). Immunohistochemistry revealed proliferation of the influenza (A/H1N1pdm) virus in alveolar epithelial cells, some of which expressed SAα2-3Gal on the cell surface. Influenza (A/H1N1pdm) virus genomic RNA and mRNA were also detected in alveolar epithelial cells. Real-time PCR revealed 723 copies/cell in the left lower lung section from which the influenza (A/H1N1pdm) virus was isolated. Electron microscopic analysis revealed filamentous viral particles in the lung tissue. The concentrations of various cytokines/chemokines in the serum and the autopsied lung tissue were measured. IL-2R, IL-6, IL-8, IL-10, IFN-α, MCP-1, and MIG levels were elevated in both. These findings indicated a case of viral pneumonia caused by influenza (A/H1N1pdm) virus infection, showing characteristic pathological findings of the early stage of DAD.

The 2009 pandemic influenza (A/H1N1pdm) virus causes severe respiratory disease, neurologic complications, and myocardial symptom in some patients (1–3). From August 15 through December 15, 2009, a total of 116 patients with confirmed infection with influenza (A/H1N1pdm) virus died in Japan (4). Autopsy verification of the cause of death is indispensable to elucidate the pathogenesis of influenza (A/H1N1pdm) virus infection. Pathological findings of fatal influenza (A/H1N1pdm) virus infection have recently been reported (5,6). Here, we report in detail the pathological and virological findings of the first autopsy case in Japan.

On August 20, 2009 (day 1), a man aged 33 years with chronic heart failure due to dilated cardiomyopathy, mild diabetes mellitus, atopic dermatitis, asthma, and obesity (BMI, 38) complained of cough and watery diarrhea. On day 6, he was admitted with progressive dyspnea, high fever (39°C) and diarrhea. On admission, a chest radiogragh showed nodular infiltrates in the lower lungs (Fig. 1a) and a chest computed tomography (CT) scan revealed severe bilateral consolidations (Fig. 1b). The leukocyte count was 5,210/mm^3 and CRP was 1.1 mg/dl. The nasopharyngeal swab specimens were negative for influenza virus type A antigen by the rapid test (ESPLINE® Influenza A&B Kit; Fujirebio, Tokyo, Japan), and therefore oseltamivir was not administered. On the morning of day 7, the patient required intubation and was placed on mechanical ventilation. At intubation, foamy, white and partly bloody fluid spouted out from the tube. Methylprednisolone pulse therapy and administration of a neutrophil elastase inhibitor (sivelestat sodium hydrate) were initiated for the treatment of acute respiratory distress syndrome (ARDS). The diagnosis of influenza (A/H1N1pdm) virus infection was confirmed by real-time reverse transcriptase-polymerase chain reaction (RT-PCR) testing on day 7. In spite of intensive care, the patient died of respiratory failure and multiple organ dysfunction syndrome on day 8. The chest radiograph showed progressive and confluent consolidations (Fig. 1c).

Autopsy revealed macroscopically severe pulmonary edema, hemorrhage, exudation and focal nodular lesions in the lungs (left, 730 g; right, 800 g) (Fig. 2a). The bilateral main bronchi were filled with foamy liquid, which was positive for influenza virus A antigen. The nodular lesions were palpable in the lower lungs, and corresponded to the nodular shadows of the chest radiographic findings (Fig. 1c). The heart was enlarged and all chambers were dilated (670 g), and the left ventricular wall and septal wall had irregular whitish patches, compatible with dilated cardiomyopathy (Figs. 2b and c). The brain was edematous and swollen (1,350 g). Hyperplastic solitary lymph follicles of the terminal ileum and rectal erosion were observed.

Tissue samples from all major organs were fixed in 20% buffered formalin and embedded in paraffin by an automated

*Corresponding author: Mailing address: Department of Pathology, National Institute of Infectious Diseases, 1-23-1 Toyama, Shinjuku-ku, Tokyo 162-8640, Japan. Tel: +81-3-5285-1111, Fax: +81-3-5285-1189, E-mail: tsata@nih.go.jp

processor (SAKURA ETV-150CV; Sakura Finetek Japan, Tokyo, Japan). Each section was cut into 3 μm in thickness, mounted on silane-coated slides (Matsunami, Tokyo, Japan) and was examined histologically. Hematoxylin and eosin-stained lung sections demonstrated intra-alveolar edema with fibrin, erythrocytes and desquamated epithelial cells in alveolar spaces, hyperplasia of type II pneumocytes, and hemosiderin-laden macrophages (heart failure cells) (Figs. 3a, b, c, d, and e). No viral inclusion bodies or cytopathic changes were observed in pneumocytes. Neutrophil infiltration was not prominent. Regenerative hyperplasia and desquamation of the pseudostratified columnar epithelium of the bronchi were observed (Fig. 3a). Some sections demonstrated the feature of early exudative-stage diffuse alveolar damage (DAD) with hyaline membrane formation (Fig. 3c). The findings of more progressed proliferative-stage DAD were also observed in a few sections (Fig. 3e).

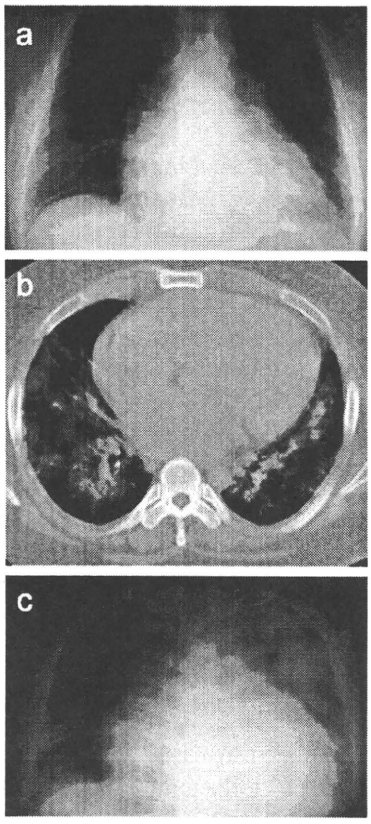

Fig. 1. Radiograph of the lung and chest computed tomography (CT). (a) The radiograph showed nodular infiltrates in lower lungs on day 6. (b) The chest CT scan revealed severe bilateral consolidations on day 6. (c) The radiograph showed progressive and confluent consolidations on day 8.

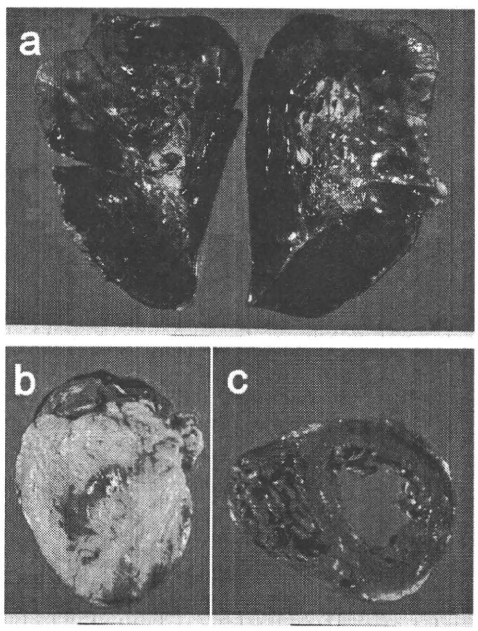

Fig. 2. Macroscopical findings. (a) Plumonary edema (left, 730 g; right, 800 g). (b, c) Enlarged heart (670 g) and dilated chambers compatible with dilated cardiomyopathy.

To evaluate the distribution of influenza (A/H1N1pdm) virus antigen, all sections were immunostained by an avidin-biotin complex immunoperoxidase method (LSAB2 kit/HRP/DAB; Dako Cytomation, Copenhagen, Denmark) using a mouse monoclonal antibody against influenza A nucleoprotein (InfA-NP) (7). Positive signals for InfA-NP antigen were detected primarily in the lung field sections, and only sparsely in a bronchial section (Figs. 3f, g, h, and i). No signals were detected in a trachea section or the other extrapulmonary tissue sections. Many viral antigen-positive cells were detected in the earlier-stage DAD lesions before hyaline membrane formation (Figs. 3f, g, h, and i) rather than in the progressed lesions (Fig. 3j). The signals were found in alveolar epithelial cells, both type I and type II pneumocytes (Figs. 3b, d, g, and i). The influenza (A/H1N1dm) virus genomic RNA (minus-strand RNA) and mRNA (plus-strand RNA) were detected in the same lesion by the in situ hybridization AT-tailing CSA (ISH-AT-CSA) method using strand-specific oligonucleotide probes for the NP region of the influenza (A/H1N1pdm) virus (sense probe: 5′-gcaaggttcaacacttcccagaaggtctggtgccgcaggt-ATATATATATATATATATATAT-3′, anti-sense probe: 5′-acctgcgg caccagaccttctgggaagtgttgaaccttgc-ATATATATATATATATATAT AT-3′) (Figs. 4a and b) (8,9). This revealed that the virus had replicated in the alveolar epithelial cells. No signals were detected using an irrelevant probe as a negative control (Fig. 4c).

To characterize the virus-infected cells, confocal laser scanning microscopy was used to visualize double immunofluorescence staining for InfA-NP and for the cell type-specific marker proteins EMA (epithelial cells), SP-D (type II pneumocytes), cytokeratin AE1/AE3 (epithelial cells), CD68 (macrophages) and CD34 (endothelial cells) as previously described (10). Alexa Fluor 568-conjugated anti-mouse or anti-rabbit IgG (Molecular Probes, Eugene, Oreg., USA) and Alexa Fluor 488-conjugated anti-rabbit or anti-mouse IgG (Molecular Probes) were used as secondary antibodies. Almost all InfA-NP signals were detected in epithelial (EMA-positive) cells (Fig. 4d). They were also detected in SP-D-positive cells, suggesting type II pneumocytese (Fig. 4e). A few were detected in AE1/AE3-positive bronchial epithelial cells. None were detected in CD68-positive macrophages or CD34-positive endothelial cells (data not shown).

The influenza A virus binds to receptors containing terminal sialic acids linked to galactose on cell surface glycoproteins by a 2-3 linkage (SAα2-3Gal) and/or by a 2-6 linkage (SAα2-6Gal) (11). Swine influenza HA binds to both SAα2-6Gal and SAα2-3Gal (12). In the human respiratory organs, putative SAα2-6Gal receptors were mainly expressed in the epithelium of the upper respiratory tract and SAα2-3Gal receptors were expressed in the epithelium of the lower respiratory tract (data not shown). The sections were incubated

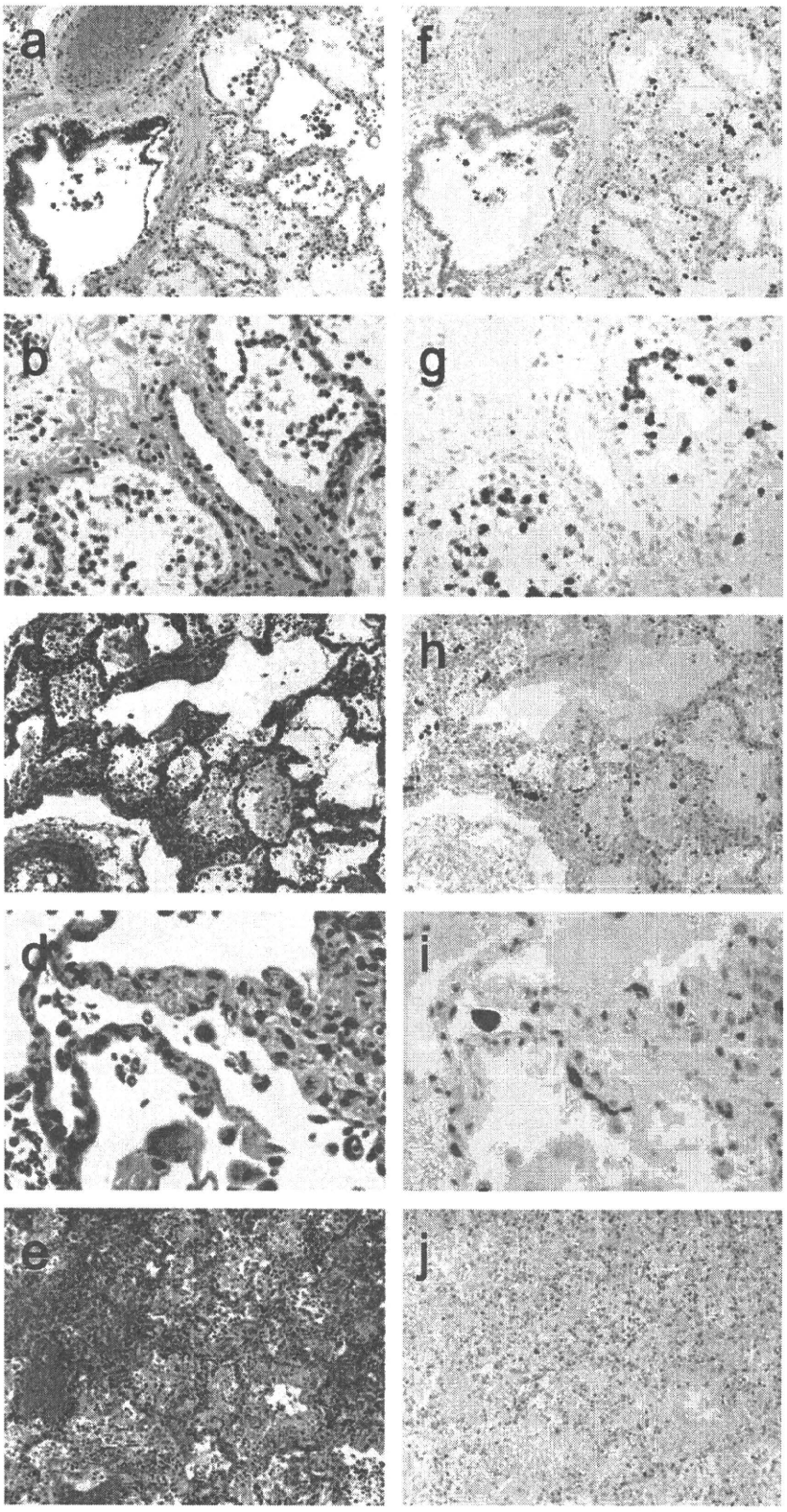

Fig. 3. Hematoxylin and eosin staining (a, b, c, d, and e) and immunohistochemistry for influenza A nucleoprotein (InfA-NP) (f, g, h, i, and j). Intra-alveolar edema with liquid, fibrin, erythrocytes and desquamated epithelial cells in alveolar spaces, hyperplasia of type II pneumocytes, and hemosiderin-laden macrophages (heart failure cells) were generally observed. (a) Regenerative hyperplasia and desquamation of the pseudostratified columnar epithelium of the bronchi were observed. (b, c, d) Early exudative-stage diffuse alveolar damage (DAD) with hyaline membrane formation. (c) More progressed proliferative-stage DAD were shown. (f, g, h, and i) A lot of viral antigen-positive cells were detected in the earlier-exudative stage DAD lesions before hyaline membranes formation. (i) The signals were also found in alveolar type I pneumocytes. (j) Few viral antigen-positive cells were detected in the progressed lesion. Original magnification, ×100 (a, c, e, f, h, and j), ×200 (b, g), ×400 (d, i).

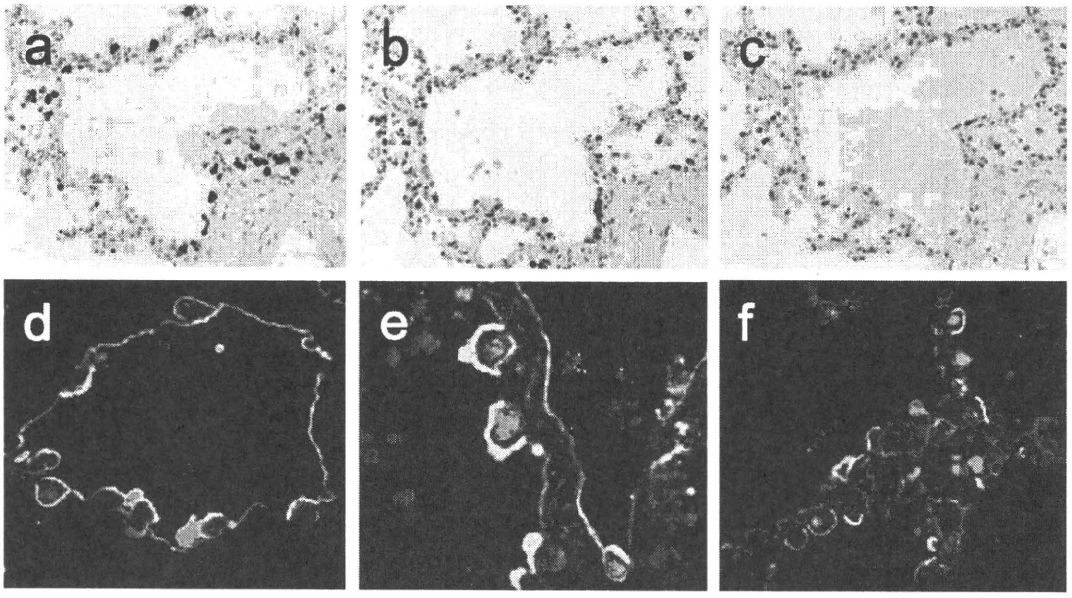

Fig. 4. The detections of influenza (A/H1N1pdm) virus-RNA using in situ hybridization AT-tailing-CSA method. (a) The influenza (A/H1N1pdm) virus genomic-RNA detected using a sense-probe. (b) The influenza (A/H1N1pdm) virus-mRNA detected using an anti-sense probe. (c) No signals were detected using an irrelevant probe. Original magnification, ×200. Double immunofluorescence staining. (d) Influenza virus A nucleoprotein (InfA-NP) (red) and EMA for epithelial cells (green) were co-localized. (e) InfA-NP (red) and SP-D for type II pneumocytes (green) were co-localized. (f) InfA-NP (red) were detected in the cells expressing sialic acids linked to galactose by a 2-3 linkage (SAα2-3Gal) (green). Original magnification, ×400.

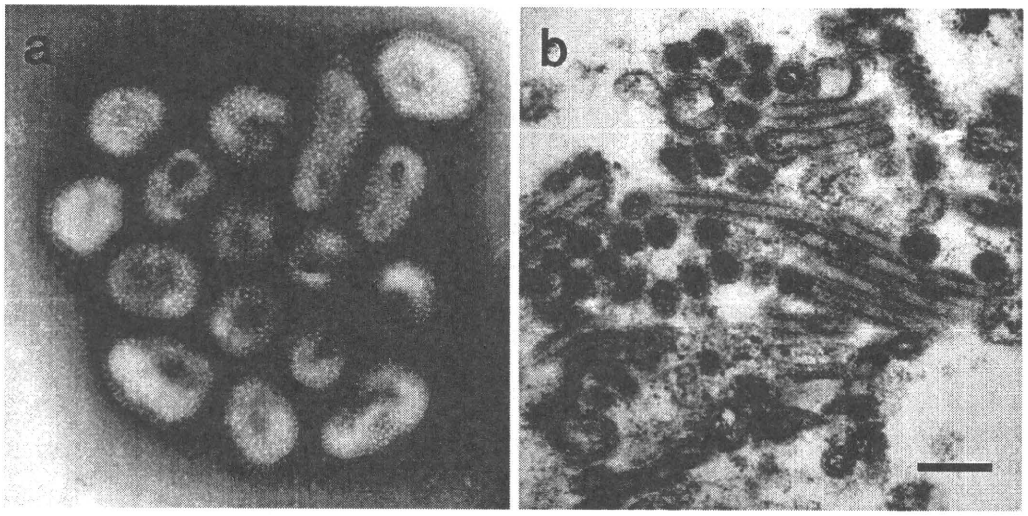

Fig. 5. Electron microscopy. (a) The negative staining feature of isolated influenza (A/H1N1pdm) virus particles in the culture supernatant. Scale bar, 100 nm. (b) The influenza (A/H1N1pdm) viral particles in filamentous forms in the lung sections. Scale bar, 200 nm.

with biotinylated-*Maackia amurensis* lectin II (MAA-II) (Vector Laboratories, Burlingame, Calif., USA) to detect SAα2-3Gal and with biotinylated-*Sambucus nigra* lectin I (SNA-I) (EY Laboratories, San Mateo, Calif., USA) to detect SAα2-6Gal. They were then incubated with Fluor 488-conjugated streptavidin (Molecular Probes). Double fluorescence staining and visualization with a confocal laser scanning microscope revealed that some infA-NP-positive cells expressed SAα2-3Gal on the cell surface (Fig. 4f), suggesting that A/H1N1pdm HA is able to bind to SAα2-3Gal receptors and to infect type II pneumocytes. Because few infA-NP are detected in bronchial epithelial cells on day 8 in this case, it was difficult to confirm that A/H1N1pdm HA was able to bind to SAα2-6Gal receptors, which are abundant on the surface of bronchial epithelial cells.

To examine the copy numbers of the influenza (A/H1N1pdm) virus, RNAs extracted from 4 paraffin-embedded sections (5 μm × 3) (left upper lung, left lower lung, left bronchus, middle trachea) were identified by quantitative real-time RT-PCR using an Mx3005P system (Stratagene, La Jolla, Calif., USA), which amplified a segment within the HA region of the A/H1N1pdm virus-RNA (13). The amount of human beta-actin mRNA in the DNase-treated RNA extracted from each section was also determined as an internal reference gene to provide a normalization factor for the amount of RNA isolated from a specimen (14). To amplify A/H1N1pdm-HA, forward (swH1N1-HA-F: 5′-CCCCATTGCA TTTGGGTAAA-3′) and reverse (swH1N1-HA-R: 5′-TGGA GAGTGATTCACACTGGAT-3′) primers were used with a labeled probe 5′-(FAM)AACATTGCTGGCTGGATCCTG

GGA(TAMRA)-3′. Real-time RT-PCR revealed 2.37×10^5 copies of A/H1N1pdm-RNA and 4.92×10^5 copies of beta-actin mRNA in the left lower lung section. The beta-actin mRNA copy number was 1,500 copies/cell (unpublished data). Therefore the influenza (A/H1N1pdm) virus-RNA copy number was calculated as 723 copies/cell in the left lower lung section. Similarly, it was calculated as 10 copies/cell in the left upper lung section, 2 copies/cell in the left bronchus and less than 1 copy/cell in the middle trachea. The differences in the copy numbers of influenza (A/H1N1pdm) virus-RNA among the sections were consistent with the differences in the numbers of InfA-NP-antigen-positive cells detected by immunohistochemistry.

A/H1N1pdm virus was isolated by inoculating 20% (w/v) homogenates of the autopsy lung tissue to Madin-Darby canine kidney (MDCK) cells in the presence of trypsin. The culture supernatants were harvested on the 3rd day post-inoculation as a stock virus. The virus titer, which was expressed as 50% of the tissue culture infectious dose ($TCID_{50}$)/ml on MDCK cells, was 7.5×10^5 $TCID_{50}$/ml. The whole sequence of the influenza virus proliferated in the lung was determined directly using an Illumina Genome Analyzer II (Illumina, San Diego, Calif., USA) and indirectly using the isolated strain. Both sequences mostly coincided with that of A/H1N1pdm. The former sequence was named A/Nagano/RC1-L/2009(H1N1) and the latter one was named A/Nagano/RC1/2009(H1N1). The negative staining feature of isolated A/H1N1pdm virus particles in the culture supernatant by electron microscopy (EM) is shown in Fig. 5a. In the lung tissue processed routinely for EM (15), outside of type II alveolar epithelial cells, influenza virus particles in filamentous rather than spherical forms were found (Fig. 5b).

The concentration of various cytokines/chemokines in the serum on day 5 and the autopsied lung tissue were measured by using a Human Cytokine 25-plex (BioSource International, Inc., Carmarillo, Calif., USA) and Luminex100TM (Luminex Co., Austin, Texas, USA) as described previously (16). IL-2R, IL-6, IL-8, IL-10, IFN-α, MCP-1, and MIG levels were elevated both in the serum on day 5 before corticosteroid treatment and the autopsy lung tissue on day 8. In addition to these data, an increase of IP-10 was observed in the serum and an increase of IFN-γ was detected in the lung tissue.

The patient had multiple risk factors for severe complications of influenza (A/H1N1pdm) virus infection, suggesting that he died of respiratory failure due to severe pulmonary edema caused by both chronic heart failure and influenza pneumonia. The lung sections showed very early exudative-stage DAD before hyaline membrane formation. Unexpectedly, a high level of proliferation of influenza (A/H1N1pdm) virus was detected in alveolar epithelial cells by immunohistochemistry, as shown in Fig. 3. We were able to detect this early stage of the disease even in the autopsied lung sections. This case provide clues to the pathogenesis of influenza pneumonia and suggests what occurs in the lungs after influenza (A/H1N1pdm) virus infection.

ACKNOWLEDGMENTS

This study was supported by the Health and Labour Sciences Research Grants on Emerging and Re-emerging Infectious Diseases (to TS and NN, No. H20-Shinko-Ippan-006 and H19-Shinko-Ippan-005) from the Ministry of Health, Labour and Welfare of Japan.

We thank Drs. Takahiro Tsuji, Naoko Iwata, and Yuko Sasaki for their technical assistance, and Dr. Toshio Kumasaka for valuable discussions.

REFERENCES

1. Centers for Disease, Control and Prevention (2009): Intensive-care patients with severe novel influenza A(H1N1) virus infection—Michigan. Morbid. Mortal. Wkly. Rep., 58, 749–752.
2. Centers for Disease, Control and Prevention (2009): Neurologic complications associated with novel influenza A (H1N1) virus infection in children—Dallas, Texas. Morbid. Mortal. Wkly. Rep., 58, 773–778.
3. Perez-Padilla, R., de la Rosa-Zamboni, D., Ponce de Leon, S., et al. (2009): Pneumonia and respiratory failure from swine-origin influenza A (H1N1) in Mexico. N. Engl. J. Med., 361, 680–689.
4. Ministry of Health, Labour and Welfare, Japan: Situation of H1N1 in Japan. Online at <http://www.mhlw.go.jp/za/0806/c17/c17.html>.
5. Mauda, T., Hajjar, L.A., Callegari, G.D., et al. (2010): Lung pathology in fatal novel human influenza A (H1N1) infection. Am. J. Respir. Crit. Care Med., 181, 72–79.
6. Gill, J.R., Sheng, Z.M., Ely., S.F., et al. (2010): Pulmonary pathologic findings of fatal 2009 pandemic influenza A/H1N1 viral infections. Arch. Pathol. Lab. Med., 134 (published on line).
7. Chen, Z., Sahashi, Y., Matsuo, K., et al. (1998): Comparison of the ability of viral protein-expressing plasmid DNAs to protect against influenza. Vaccine, 16, 1544–1549.
8. Nakajima, N., Ionescu, P., Sato, Y., et al. (2003): In situ hybridization AT-tailing with catalyzed signal amplification for sensitive and specific in situ detection of human immunodeficiency virus-1 mRNA in formalin-fixed and paraffin-embedded tissues. Am. J. Pathol., 162, 381–389.
9. Nakajima, N., Asahi-Ozaki, Y., Nagata, N., et al. (2003): SARS coronavirus-infected cells in lung detected by new in situ hybridization technique. Jpn. J. Infect. Dis., 56, 139–141.
10. Liem, N.T., Nakajima, N., Phat, L.P., et al. (2008): H5N1-infected cells in lung with diffuse alveolar damage in exudative phase from a fatal case in Vietnam. Jpn. J. Infect. Dis., 61, 157–160.
11. Shinya, K., Ebina, M., Ono, M., et al. (2006): Avian flu: influenza receptors in the human airway. Nature, 440, 435–436.
12. Gambaryan, A.S., Tuzikov, A.B., Piskarev, V.E., et al. (1997): Specification of receptor-binding phenotypes of influenza virus isolates from different hosts using synthetic sialyglycopolymers: non-egg-adapted human H1 and H3 influenza A and influenza B viruses share a common high binding affinity for 6′-sialyl (*N*-acetyllactosamine). Virology, 232, 345–350.
13. Katano, H., Ito, H., Suzuki, Y., et al. (2009): Detection of Merkel cell polyomavirus in Merkel cell carcinoma and Kaposi's sarcoma. J. Med. Virol., 81, 1951–1958.
14. Kuramochi, H., Hayashi, K., Uchida, K., et al. (2006): Vascular endothelial growth factor messenger RNA expression level is preserved in liver metastases compared with corresponding primary colorectal cancer. Clin. Cancer Res., 12, 29–33.
15. Tobiume, M., Sato, Y., Katano, H., et al. (2009): Rabies virus dissemination in neural tissues of autopsy cases due to rabies imported into Japan from Philippines: immunohistochemistry. Pathol. Int., 59, 555–566.
16. Nagata, N., Iwata, N., Hasegawa, H., et al. (2008): Mouse-passaged severe acute respiratory syndrome-associated coronavirus leads to lethal pulmonary edema and diffuse alveolar damage in adult but not young mice. Am. J. Pathol., 172, 1625–1637.

Characterization of Quasispecies of Pandemic 2009 Influenza A Virus (A/H1N1/2009) by *De Novo* Sequencing Using a Next-Generation DNA Sequencer

Makoto Kuroda[1]*, Harutaka Katano[2], Noriko Nakajima[2], Minoru Tobiume[2], Akira Ainai[2], Tsuyoshi Sekizuka[1], Hideki Hasegawa[3], Masato Tashiro[3], Yuko Sasaki[4], Yoshichika Arakawa[4], Satoru Hata[5], Masahide Watanabe[6], Tetsutaro Sata[2]

1 Laboratory of Bacterial Genomics, Pathogen Genomics Center, National Institute of Infectious Diseases, Tokyo, Japan, **2** Department of Pathology, National Institute of Infectious Diseases, Tokyo, Japan, **3** Influenza Virus Research Center, National Institute of Infectious Diseases, Tokyo, Japan, **4** Department of Bacterial Pathogenesis and Infection Control, National Institute of Infectious Diseases, Tokyo, Japan, **5** Department of Clinical Laboratory, Nagano Red Cross Hospital, Nagano, Japan, **6** Department of Pathology, Nagano Red Cross Hospital, Nagano, Japan

Abstract

Pandemic 2009 influenza A virus (A/H1N1/2009) has emerged globally. In this study, we performed a comprehensive detection of potential pathogens by *de novo* sequencing using a next-generation DNA sequencer on total RNAs extracted from an autopsy lung of a patient who died of viral pneumonia with A/H1N1/2009. Among a total of 9.4×10^6 40-mer short reads, more than 98% appeared to be human, while 0.85% were identified as A/H1N1/2009 (A/Nagano/RC1-L/2009(H1N1)). Suspected bacterial reads such as *Streptococcus pneumoniae* and other oral bacteria flora were very low at 0.005%, and a significant bacterial infection was not histologically observed. *De novo* assembly and read mapping analysis of A/Nagano/RC1-L/2009(H1N1) showed more than ×200 coverage on average, and revealed nucleotide heterogeneity on hemagglutinin as quasispecies, specifically at two amino acids (Gly_{172}Glu and Gly_{239}Asn of HA) located on the Sa and Ca2 antigenic sites, respectively. Gly239 and Asn239 on antigenic site Ca2 appeared to be minor amino acids compared with the highly distributed Asp239 in H1N1 HAs. This study demonstrated that *de novo* sequencing can comprehensively detect pathogens, and such in-depth investigation facilitates the identification of influenza A viral heterogeneity. To better characterize the A/H1N1/2009 virus, unbiased comprehensive techniques will be indispensable for the primary investigations of emerging infectious diseases.

Citation: Kuroda M, Katano H, Nakajima N, Tobiume M, Ainai A, et al. (2010) Characterization of Quasispecies of Pandemic 2009 Influenza A Virus (A/H1N1/2009) by *De Novo* Sequencing Using a Next-Generation DNA Sequencer. PLoS ONE 5(4): e10256. doi:10.1371/journal.pone.0010256

Editor: Steven Jacobson, National Institutes of Health, United States of America

Received February 19, 2010; **Accepted** March 27, 2010; **Published** April 23, 2010

Funding: This work was supported by grants for Research on Emerging and Re-emerging Infectious Diseases (H20 and 21 Shinko-Ippan-6), from the Ministry of Health, Labour, and Welfare, Japan. The funders had no role in study design, data collection and analysis, decision to publish, or preparation of the manuscript.

Competing Interests: The authors have declared that no competing interests exist.

* E-mail: makokuro@nih.go.jp

Introduction

In April 2009, an H1N1 triple-reassortant swine influenza virus (A/H1N1/2009) was detected in humans with febrile respiratory illness in North America [1], and the virus has rapidly spread worldwide by human-to-human transmission. According to the disease outbreak news from the World Health Organization, at least 14,711 people died from A/H1N1/2009 between April 2009 and January 2010 (http://www.who.int/csr/don/en/). Fatal cases from A/H1N1/2009 viral infection were summarized in a report by Gill *et al.* [2].

The genome of influenza A virus (family Orthomyxoviridae) consists of 8 single-stranded negative sense RNA molecules spanning approximately 13.5 kb. The segments range in length from 890 to 2341 nucleotides (nt) and encode a total of 11 proteins [3]. Genetic diversity in influenza virus results from a high mutation rate associated with replication using a low-fidelity RNA polymerase and the reshuffling (reassortment) of segments among coinfecting strains. Multiple-reassortant influenza viruses from avian, human, and swine origins emerged as major pandemic influenza viruses (i.e., 1918 H1N1, 1957 H2N2, and 1968 H3N2) causing significant mortality in humans in the 20th century [4]. Such an "antigenic shift" by multiple reassortant drives the emergence of pandemic influenza viruses, with their severity and clinical outcome always unpredictable [5].

Influenza A virus can evade antibodies specific to its attachment protein, hemagglutinin (HA), by the accumulation of amino acid substitutions in HA epitopes [6]. This "antigenic drift" in HA epitopes [7] affects recognition by antibodies that neutralize viral infectivity by blocking the interaction of HA with sialic acid residues on host-cell membranes. The H1 subtype HA has four antigenic sites recognized by monoclonal antibodies with high neutralizing activity, designated Sa, Sb, Ca, and Cb [8]. In addition, 8 continuous B cell/antibody epitopes for human H1N1 HA proteins have been experimentally defined by the Immune Epitope Database and Analysis Resource (IEDB: http://www.immuneepitope.org/) [9]. Immune epitope analysis of HA epitopes in A/H1N1/2009 is also summarized in the Influenza Research Database (http://www.fludb.org/brc/homeExtraPage.do?decorator=influenza&extraPage=separate) [10].

To better predict a future pandemic of influenza A virus, the characterization of possible antigenic drift will be indispensable. Igarashi *et al.* and Shen *et al.* reported that a structural comparison of HAs could predict probable future antigenic changes during the evolution of A/H1N1/2009 in the human population [11,12].

In addition to this prediction, extensive investigations on viral quasispecies will be required to reveal the actual appearance of those antigenic changes. Nakamura *et al.* demonstrated the direct detection of potential pathogens, including influenza virus, using *de novo* pyrosequencing [13], but the detection appeared to have insufficient redundant sequencing reads to reveal the genetic variation of the viruses. Ramakrishnan *et al.* demonstrated the discrimination of quasispecies in mixed HA subtype infections of influenza A virus using the same pyrosequencing approach [14]. However, it was shown that the influenza viral RNA sample should be enriched through sequence-specific oligonucleotide capturing prior to pyrosequencing, indicating that such enrichment might represent a biased result.

Here, we performed *de novo* sequencing using total RNAs extracted from an autopsy lung of a patient infected with A/H1N1/2009, and detected potential pathogens such as bacteria in addition to A/H1N1/2009. Extensive DNA sequencing using the Illumina Genome Analyzer II (GA II) revealed that quasispecies for the HA sequence were generated in single patient. Such heterogeneity demonstrated the antigenic drift of HA, implying the existence of a mechanism to escape pre-existing human immunity to the virus.

Results

Summary of sequencing reads and detection of potential pathogens

To determine the influenza A virus sequence and other potential pathogens, we performed *de novo* sequencing of double-stranded cDNA from total RNA extracted from the autopsy lung of a patient infected with the A/H1N1/2009 virus (A/Nagano/RC1/2009(H1N1)) in August 2009 in Japan. The patient was found to be positive for A/H1N1/2009 by real-time reverse transcriptase-polymerase chain reaction (RT-PCR); histopathological findings were also reported [15]. GA II produced 9.4×10^6 40-mer reads from the cDNA library (Fig. 1B). To exclude the human-derived read sequences, we performed an analysis pipeline as follows (Fig. 1A). Initially, all 9,475,890 reads were aligned to a reference sequence of human genomic DNA, followed by quality trimming to remove low-quality reads and excluding reads with similarities to ambiguous human sequences, resulting in 9,309,538 reads (98.24%) with a possible human source (Fig. 1B). The remaining 166,352 reads (1.75%) were further analyzed using a BLAST search against non-redundant databases, revealing 80,827 (0.85%), 469 (0.005%), and 85,056 (0.90%) reads as influenza A virus, bacteria, and no hits, respectively (Fig. 1B).

Regarding the bacterial hits, species classification was determined based on the results of a BLASTN search against the nt database (Fig. 1C). The most abundant bacterium was *Propionibacterium acnes*, but our other sequencing trials for clinical specimens suggest that this species is always detected (data not shown). Therefore, the presence of *P. acnes* could be the result of contamination at some point from the autopsy to the preparation of the cDNA library. In addition to *P. acnes*, *Escherichia coli* and *Acinetobacter baumannii* were frequently detected as possible contaminants. Suspected bacterial pathogens were identified as *Streptococcus pneumoniae* and *Porphyromonas gingivalis*. Specific PCR using 16S-rDNA and the *lytA* gene was performed for further verification of the presence of *S. pneumoniae* (data not shown). Although *S. pneumoniae* was not sufficiently abundant to conclude a coinfection with A/H1N1/2009, the severity of the A/H1N1/2009 infection could be correlated with *S. pneumoniae*, as reported by Palacios *et al* [16]. The other detected bacteria, such as *Streptococcus* sp., generally constitute the normal human oral flora.

de novo assembly of the A/H1N1/2009 virus

Whole 40-mer short reads, including human-derived reads, were assembled using Euler-SR or the Velvet *de novo* assembler. The resultant contigs generated using Euler-SR had longer extended sequences than those generated using Velvet (data not shown); thus, all further analyses were performed using the contigs generated using Euler-SR (Texts S1 and S2). All contigs showed high similarity to the sequences of A/H1N1/2009 (Table 1). Among the 8 segments, almost the whole lengths of segments 2 (2321 nt), 3 (2231 nt), 4 (1765 nt), 5 (1562 nt), 7 (1026 nt), and 8 (892 nt) were correctly assembled as single contigs of 2204, 2198, 1761, 1514, 1019, and 834 nt, respectively (Table 1 and Fig. 2). Segments 1 and 6 were divided into several contigs, but were correctly aligned to the known sequences (Table 1 and Fig. 2).

Read mapping analysis of the A/H1N1/2009 virus

To obtain whole sequences and identify single nucleotide polymorphisms (SNPs) for the 8 segments, the 40-mer short reads were aligned to the sequence of A/Tronto/T0106/2009(H1N1), which was found to be the most similar to the A/H1N1/2009 virus using a BLASTN search. Figure 2 shows dot plot images of the coverage at every nucleotide of the segments. Read coverage was observed at $\sim\times200$ on average for all segments, indicating a sufficient redundancy to identify the viral sequences and SNPs. The obtained viral sequences, designated as A/Nagano/RC1-L/2009(H1N1), were consistent with those from A/Nagano/RC1/2009(H1N1) passaged in the Madin-Darby canine kidney (MDCK) cell line, except for 3 possible heterogeneous nucleotides in HA.

The coverage plot curves were not flat throughout the segments. Intriguingly, both ends of segment 1 (encoding PB2), the 3′–end of segment 3 (encoding PA), and approximately 700 nt of segment 8 (encoding NS) showed significant abundant coverage greater than $\times1000$.

Genetic population analysis of the A/H1N1/2009 virus

To identify heterogeneous populations, alignment results were screened using MapView software (Fig. 3B). Three potential heterogeneous genetic populations were found in segment 4 (encoding HA) at the 515, 715, and 716 nt positions (Fig. 3A), but not in other segments. The read alignments shown in Fig. 3B indicate that either the GGT or AAT sequence appeared at the 715–717 nt position, but not the GAT or AGT sequence. In addition, the read coverage implied that the major (GG; HA-Major) or minor (AA; HA-Minor) nucleotides were detected at the frequencies of 75% and 25%, respectively. To validate these variations, HA-Major- or HA-Minor-specific quantitative RT-PCR (qRT-PCR) was performed for the preparation of specific PCR products between the 434 and 738 nt in the HA coding sequence (Fig. 3C). qRT-PCR demonstrated that the expression of HA was ~40,000-fold greater than that of human β-actin, and the expression ratio of HA-Major/HA-Minor was 4.05, suggesting that it corresponds to the read mapping shown in Fig. 3A. Furthermore, HA-Major and HA-Minor sequences were verified by Sanger DNA sequencing of the specific PCR products (Fig. 3D). Taken together, these results suggest the following amino acid substitutions of HA: one nucleotide alteration causes $Gly_{172}Glu$ and the other two alterations cause $Gly_{239}Asn$ (Fig. 3D).

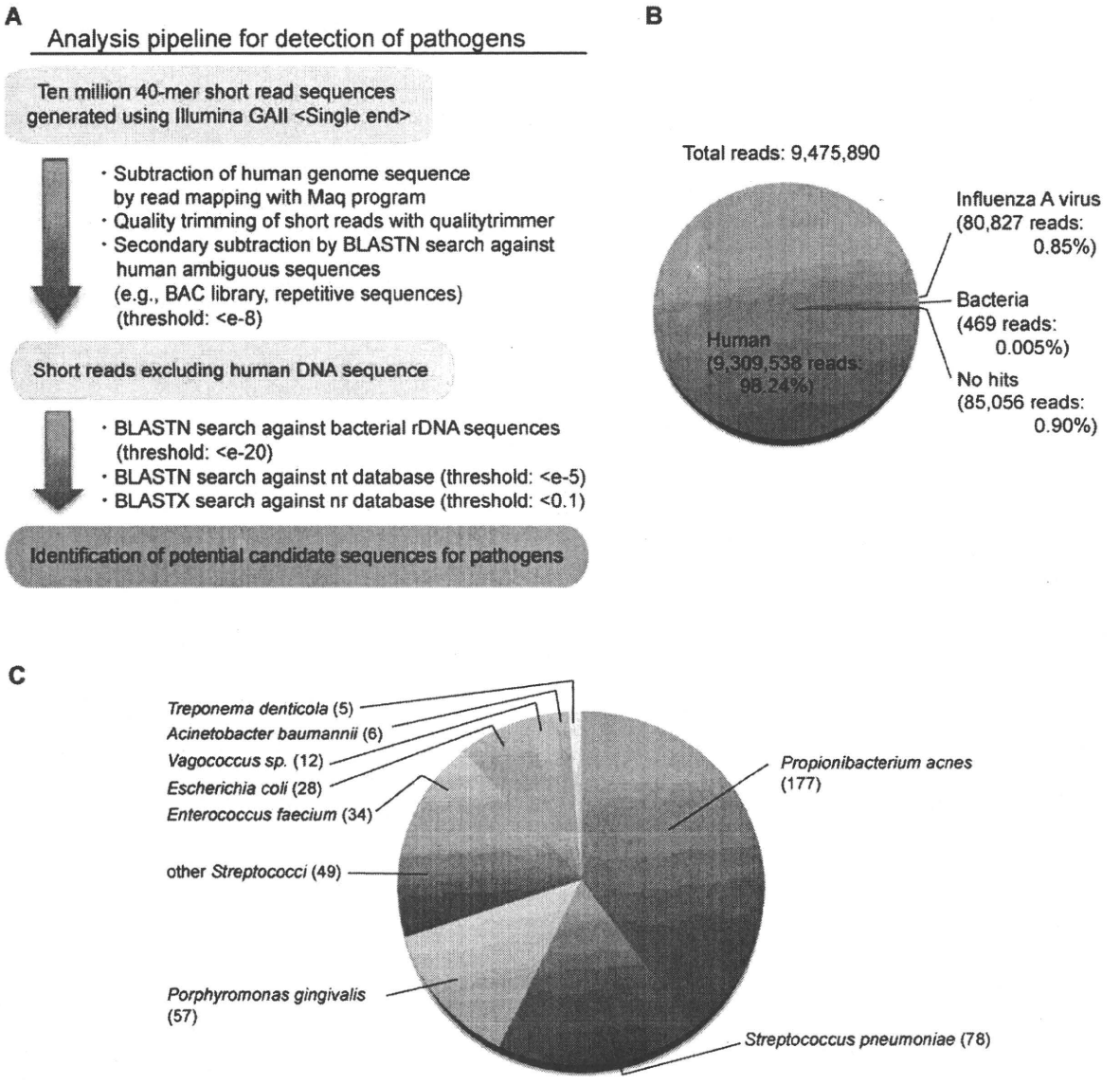

Figure 1. Detection of potential pathogens by comprehensive *de novo* sequencing. (**A**) Schematic representation of the analysis pipeline for the detection of pathogens from comprehensive sequencing of human clinical specimens. After excluding human-derived DNA sequences using Maq software and a BLAST homology search against human genomic DNA and human ambiguous sequences extracted from the nt database, the remaining short reads were subjected to a BLAST search to detect potential pathogens. (**B**) Pie chart of the homology search results for the 40-mer short reads. Read numbers and their percentage to the total reads are shown in parenthesis. (**C**) Pie chart of identified bacterial hits. Number of hit reads is shown in parenthesis. Bacteria with less than 5 hit reads were excluded.
doi:10.1371/journal.pone.0010256.g001

Epitope analysis of heterogeneous HA

To elucidate whether the $Gly_{172}Glu$ and $Gly_{239}Asn$ amino acid substitutions in the HA sequence could be associated with antigenic drift, they were compared to known potential epitopes [8,9]. Representative HA amino acid sequences of the H1N1 influenza A virus were aligned with the heterogeneous HA-Major and HA-Minor sequences. The $Gly_{172}Glu$ substitution (corresponding to Gly158 in the mature HA lacking a signal peptide) was located on the Sa antigenic site (Fig. 4A).

The HA $Gly_{172}Glu$ substitution is likely to be rare thus far because a BLASTP search against the non-redundant nr database revealed only two identical hits, A/Bayern/62/2009(H1N1) in Germany and A/Catalonia/S1207/2009(H1N1) in Spain (data not shown). One intriguing hit was to A/Pennsylvania/14/2009(H1N1) isolated in the US, whose HA sequence has an Xaa amino acid at position 172 due to the presence of the heterogeneous nucleotide R (A or G) (Fig. 5A). This deposited sequence completely coincides with our observation, suggesting that two variants of HAs are likely to coexist in the human lung, further implying that such heterogeneous populations might frequently be generated during infection.

Furthermore, HA $Gly_{239}Asn$ was located on the Ca2 antigenic site that contributes to binding with the host's sialic acid receptor [17]. Asp239 (corresponding to Asp225 in the mature HA lacking a signal peptide) was frequently distributed in H1N1 HAs (Fig. 4B), but Gly239 and Asn239 were found to be minor amino acids among HAs; a BLASTN search found 18 and 5 hit entries on the nt database, respectively. As was observed for Gly172, Xaa239

Table 1. BLASTN search results of *de novo* assembly contigs against database of Influenza virus sequences.

Euler-SR_contigs	Contig length (bp)	Virus segment	Top hit of accession number using BLASTN search against databse of Influenza virus sequences	Length of subject (bp)	Identities	Contig location for A/Toronto/T0106/2009(H1N1)
>826 183 2835	183	1	gb|GQ328865|INFLUENZA A virus (A/Finland/553/2009(H1N1)) segment 1 polymerase PB2 (PB2)	2345	167/168 (99%)	5–168
>324 1558 136	1558	1	gb|GQ365425|INFLUENZA A virus (A/Fukushima/1/2009(H1N1)) segment 1 polymerase PB2 (PB2)	2280	1556/1558 (99%)	201–1758
>1194 239 112	239	1	gb|GQ894926|INFLUENZA A virus (A/Delaware/03/2009(H1N1)) segment 1 polymerase PB2 (PB2)	2280	214/214 (100%)	1894–2107
>887 174 3294	174	1	gb|GQ894833|INFLUENZA A virus (A/Rhode Island/08/2009(H1N1)) segment 1 polymerase PB2 (PB2)	2280	156/156 (100%)	2145–2300
>890 2204 4651	2204	2	gb|GQ894924|INFLUENZA A virus (A/New Mexico/04/2009(H1N1)) segment 2 polymerase PB1 (PB1)	2274	2200/2204 (99%)	41–2244
>696 2198 3968	2198	3	gb|GQ866924|INFLUENZA A virus (A/Thailand/CU-H106/2009(H1N1)) segment 3 polymerase PA (PA)	2238	2152/2155 (99%)	54–2208
>868 1761 3831	1761	4	gb|CY045503|INFLUENZA A virus (A/Bayern/66/2009(H1N1)) segment 4 sequence	1754	1750/1754 (99%)	1–1741
>897 1514 1710	1514	5	gb|GQ502907|INFLUENZA A virus (A/Toronto/R8557/2009(H1N1)) segment 5 nucleocapsid protein	1558	1511/1514 (99%)	36–1549
>224 101 9	101	6	gb|GQ502908|INFLUENZA A virus (A/Toronto/R8557/2009(H1N1)) segment 6 neuraminidase (NA)	1458	101/101 (100%)	3–103
>1206 1302 2468	1302	6	gb|GQ906584|INFLUENZA A virus (A/Stockholm/49/2009(H1N1)) segment 6 neuraminidase (NA)	1447	1299/1300 (99%)	124–1423
>750 1019 1128	1019	7	gb|CY045957|INFLUENZA A virus (A/Toronto/T0106/2009(H1N1)) segment 7 sequence	1026	1017/1017 (100%)	9–1025
>809 834 4399	834	8	gb|GQ485660|INFLUENZA A virus (A/Ekaterinburg/01/2009(H1N1)) segment 8 nuclear export	877	828/830 (99%)	52–881

Schematic representation of contigs is shown in Fig. 2.
doi:10.1371/journal.pone.0010256.t001

was found in the nt database (Fig. 5B), suggesting that HA heterogeneity of both minor amino acids may affect its binding affinity to the sialic acid receptor.

Discussion

In this study, we demonstrated the detection of potential pathogens using a next-generation DNA sequencer. We speculated that, in addition to influenza A virus, additional potential pathogens such as *S. pneumoniae* could contribute to the severity and fatality of infection with the A/H1N1/2009 virus [2,16]. In this case, the amount of bacteria detected was small (Fig. 1B and 1C), and they were considered to be the result of contamination during the course of the experiment, from autopsy to short read sequencing. The clinical outcome of the patient and histopathological examination suggest that this was a case of influenza viral pneumonia rather than bacterial infection [15], although *S. pneumoniae* coinfection has been reported to play a crucial role in the severity of influenza virus infection in some cases [16,18].

In the present autopsy lung sample, very significant viral copies (~40,000-fold greater than β-actin) were determined using qRT-PCR, but this was not always observed in autopsy samples from other patients (less than β-actin) (data not shown). Such abundant read sequencing enabled us to obtain almost full-coverage contig sequences for the viral segments using *de novo* assembly, suggesting the importance of this result in terms of being able to evaluate uncharacterized emerging infectious agents using an unbiased sequencing technique at the outbreak of a pandemic. Indeed, this study demonstrated that whole contigs can be identified as A/H1N1/2009, but not seasonal H1N1 or other subtypes (Table 1).

The read coverage profile generated by mapping was very indicative for segment 1 encoding PB2 (Fig. 2). Both ends were highly redundant with up to ×3000 coverage. The coverage is reflected by the amounts of vRNA, cRNA, and mRNA of influenza A virus, implying that the coverage bias may detect a more stable region as it is dependent on the expression level or manner of replication.

Contrary to the viral sequences obtained for A/Nagano/RC1/2009(H1N1) isolated from passaging in MDCK cells, *de novo* sequencing revealed the presence of A/Nagano/RC1-L/2009(H1N1) HA quasispecies in the autopsy sample (Fig. 3). Despite the fact that immunity to A/H1N1/2009 viruses is supposed to be limited among the general human population [19], we detected the amino acid substitution $Gly_{172}Glu$ in the HA Sa antigenic site in A/Nagano/RC1-L/2009(H1N1), and this appears to be a very rare event among A/H1N1/2009 viruses to date.

We also observed another substitution of $Gly_{239}Asn$ in the HA Ca2 antigenic site of A/Nagano/RC1-L/2009(H1N1). This antigenic site plays a crucial role in conferring specificity to galactose of the human α2-6 sialylated glycan receptor [20]. Interestingly, Asp239 (corresponding to Asp225 in the mature HA that lacks a signal peptide) is highly prevalent in known H1N1 HAs, indicating that both Gly239 and Asn239 appear to be very minor amino acids among all HA sequences.

Thus far, amino acid substitutions in the HAs of A/H1N1/2009 have been identified compared with seasonal H1N1 HAs. Homology-based structural investigations [17,21] suggest that A/H1N1/2009 HA has the necessary residues to provide optimal contacts for high affinity binding to α2-6 sialylated glycans present

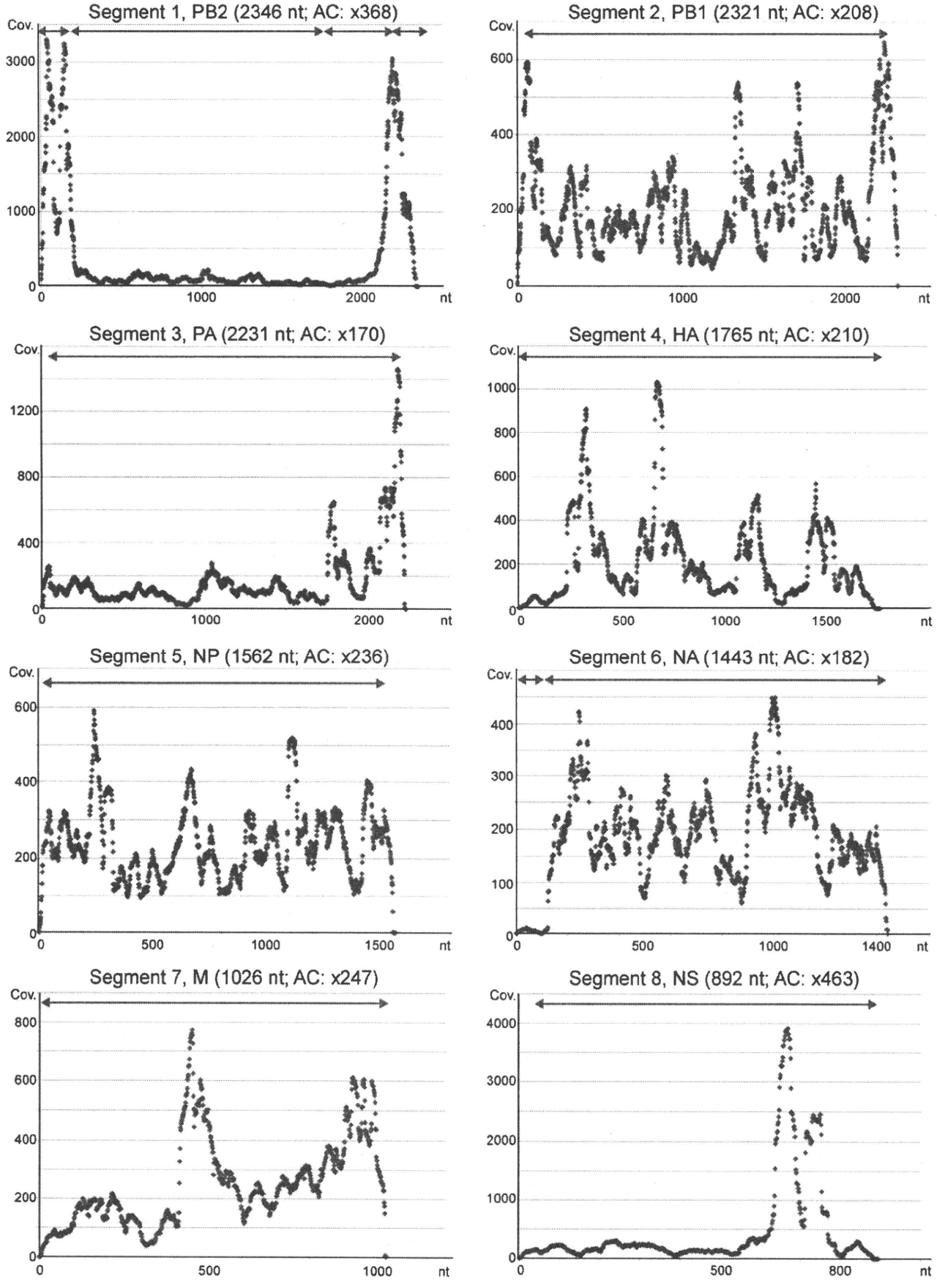
Segment 1, PB2 (2346 nt; AC: x368)
Cov.
3000
2000
1000
0
0
1000
2000
nt
Segment 2, PB1 (2321 nt; AC: x208)
Cov.
600
400
200
0
0
1000
2000
nt
Segment 3, PA (2231 nt; AC: x170)
Cov.
1200
800
400
0
0
1000
2000
nt
Segment 4, HA (1765 nt; AC: x210)
Cov.
1000
800
600
400
200
0
0
500
1000
1500
nt
Segment 5, NP (1562 nt; AC: x236)
Cov.
600
400
200
0
0
500
1000
1500
nt
Segment 6, NA (1443 nt; AC: x182)
Cov.
400
300
200
100
0
0
500
1000
1400
nt
Segment 7, M (1026 nt; AC: x247)
Cov.
800
600
400
200
0
0
500
1000
nt
Segment 8, NS (892 nt; AC: x463)
Cov.
4000
3000
2000
1000
0
0
500
800
nt